

## Author's Accepted Manuscript

Evaluation of Epoxy Crosslinking Using Ultrasonic Lamb Waves

Camille Gauthier, Jocelyne Galy, Mounsif Ech-Cherif El-Kettani, Damien Leduc, Jean-Louis Izbicki



PII: S0143-7496(17)30168-9  
DOI: <http://dx.doi.org/10.1016/j.ijadhadh.2017.09.008>  
Reference: JAAD2059

To appear in: *International Journal of Adhesion and Adhesives*

Received date: 11 May 2017  
Accepted date: 3 September 2017

Cite this article as: Camille Gauthier, Jocelyne Galy, Mounsif Ech-Cherif El-Kettani, Damien Leduc and Jean-Louis Izbicki, Evaluation of Epoxy Crosslinking Using Ultrasonic Lamb Waves, *International Journal of Adhesion and Adhesives*, <http://dx.doi.org/10.1016/j.ijadhadh.2017.09.008>

This is a PDF file of an unedited manuscript that has been accepted for publication. As a service to our customers we are providing this early version of the manuscript. The manuscript will undergo copyediting, typesetting, and review of the resulting galley proof before it is published in its final citable form. Please note that during the production process errors may be discovered which could affect the content, and all legal disclaimers that apply to the journal pertain.

## Evaluation of Epoxy Crosslinking Using Ultrasonic Lamb Waves

Camille Gauthier,<sup>a,b,c</sup> Jocelyne Galy,<sup>c</sup> Mounsif Ech-Cherif El-Kettani,<sup>a,b</sup> Damien Leduc,<sup>a,b</sup> Jean-Louis Izbicki<sup>a,b</sup>

<sup>a</sup> *Laboratoire Ondes et Milieux Complexes, UMR CNRS 6294, Université du Havre, Le Havre, France*

<sup>b</sup> *Fédération Acoustique Nord-Ouest 2, FR CNRS 3110*

<sup>c</sup> *Université de Lyon, F-69003, Lyon, France ; INSA Lyon, CNRS, UMR 5223, Ingénierie des Matériaux Polymères, F-69621, Villeurbanne, France*

Corresponding author: [elkettani@univ-lehavre.fr](mailto:elkettani@univ-lehavre.fr)

[camille.gauthier@etu.univ-lehavre.fr](mailto:camille.gauthier@etu.univ-lehavre.fr)

[jocelyne.galy@insa-lyon.fr](mailto:jocelyne.galy@insa-lyon.fr)

[damien.leduc@univ-lehavre.fr](mailto:damien.leduc@univ-lehavre.fr)

### ABSTRACT

The use of epoxy adhesives in structural bonding provides lightweight materials, however the assessment of the integrity and quality of the joint is of critical concern. Thus it is essential to know if the adhesive is well crosslinked. This work deals with the nondestructive acoustic characterization of epoxy networks, representative of the adhesive family, of different crosslinking density; i.e. conversion. Different curing cycles were applied and differential scanning calorimetry measurements allowed the determination of their glass transition temperature and epoxy conversion. The acoustic study was performed on epoxy plane plates, all in the glassy state and well beyond the gel point. The methods were based on the propagation of bulk longitudinal and shear waves, as well as on guided Lamb waves. Depending on the conversion of the epoxy, it was shown that the changes in thermo-mechanical properties, resulting from different degrees of cure, greatly influence the acoustic behavior of some Lamb modes if a selection of the sensitive modes has been performed upstream.

*Keywords:* Epoxy networks, Conversion, Ultrasounds, Lamb waves

## 1. Introduction

Epoxy networks constitute a broad class of polymeric materials with a wide range of applications, including as adhesives. However, the development of structural adhesive bonding in high-loaded structures suffers from a lack of control of the joint quality. Various nondestructive techniques (NDT) are adequate for the characterization of defects like pores, delamination, or debonding within adhesive joints, but there is so far no ultrasound NDT technique to ensure the detection of a weak bond and, by extension, to ensure the quality of an adhesive bond. The objective of our project is to develop innovative nondestructive methods sensitive to the adhesion level of an assembly, such as in aluminum-epoxy-aluminum bonds. Two well-known critical factors affecting the adhesive strength of a joint, and representative of scenarios that can happen during manufacturing are, on one hand, the surface treatment of the substrate [1] and, on the other, the epoxy conversion directly related to the curing cycle [2]. In a preliminary step of the study mechanical tests were realized on aluminum-epoxy-aluminum bonds [3],[4], and the results evidenced the effect of the epoxy adhesive conversion on the adhesive strength. A difference close to 50 % was found between a partially cured adhesive (conversion  $x=0.8$ ) and a fully cured adhesive (conversion  $x=1$ ), when using the same surface treatment of the aluminum substrate. In addition, previous studies on the influence of the epoxy conversion on the bulk properties of epoxy networks have shown that a partially cured epoxy network is far from being perfected; it has many unreacted chain ends, is more brittle than a fully cured network, and has a higher Young modulus at room temperature, lower elongation, and strain at break [5]. Unsurprisingly, these differences of mechanical behavior influence the strength of the joint.

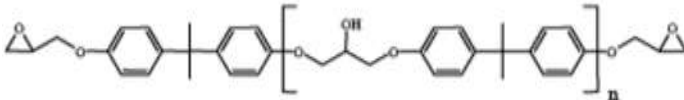
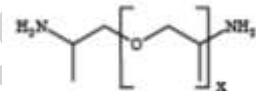
As a first step in developing innovative NDT, relying on guided wave modes to assess the level of adhesion in adhesive joints [6][10], this paper focuses on the development of a pertinent ultrasound-based method, able to evaluate the degree of crosslinking of the epoxy adhesive. Ultrasonic techniques have been used mainly to follow the kinetics of epoxy system crosslinking [11],[12], with methods based on the measurement of the ultrasonic velocity ( $v$ ) and attenuation as a function of time of reaction at a given temperature. Then, from the velocity values the elastic moduli,  $M$ , were calculated. The present paper reports the acoustic characterization of a series of glassy epoxy networks that were synthesized with different conversions. At first, differential scanning calorimetry was used to calculate precisely the epoxy conversion of networks crosslinked via different curing cycles. Then two acoustic methods, leading to the measurement of ultrasonic wave velocities, and to the plot of dispersion curves of Lamb waves, were applied with the aim of finding a pertinent parameter able to differentiate clearly the different epoxy networks.

## 2. Materials and methods

### 2.1. Materials

The epoxy adhesive used in this investigation is a two-component model system. The epoxy resin was diglycidyl ether of bisphenol A DGEBA, (DER331, Dow Chemicals), with an epoxy equivalent weight of 182–192 g/eq. The curing agent was polyetheramine (Jeffamine D230, Huntsman), with an amine equivalent weight equal to 60 g/eq. The structures of the components are shown in Table 1. The epoxy resin and the diamine curing agent were mixed mechanically in a glass reactor at room temperature, at stoichiometric ratio amino hydrogen/epoxy equal to 1. The mixture was carefully degassed under a vacuum to avoid the formation of air bubbles in the epoxy samples. Then the mixture was poured into a closed aluminum mold coated with a release agent. The thickness was controlled by the insertion of a silicone spacer of a given thickness between the two aluminum plates. The mold was placed either in a regulated room or in a regulated oven. Three curing cycles were used to crosslink the materials: the first of one week at room temperature; the second of 48 hours at room temperature, followed by two hours at 160 °C; and the third of 48 hours at room temperature, followed by three hours at 160 °C. This last curing cycle is known to lead to a fully cured network, whereas the two others lead to partially cured networks. The dimensions of the samples were 150 mm × 200 mm, with four different thicknesses: 2, 3, 4, and 5 mm.

Table 1: Chemical structure of components

Name	Chemical structure	Equivalent weight (g/eq)
DGEBA DER 331		182-192
Jeffamine D230		60

### 2.2. Methods

#### 2.2.1. Thermal characterization

Differential scanning calorimetry (DSC) measurements were taken either on the partially reacted epoxy-amine formulation, or on the cured networks. A DSC Q20 (TA Instruments) microcalorimeter was used, and the thermal properties were analyzed under an inert atmosphere at a heating rate equal to 10 °C/min. Five to ten milligrams of samples were sealed in hermetic aluminum pans. The

evolution of the glass transition temperature,  $T_g$ , and of the enthalpy of reaction,  $\Delta H$ , during the curing of the epoxy system at room temperature was followed by analyzing the samples periodically. Scans from  $-70\text{ }^\circ\text{C}$  to  $250\text{ }^\circ\text{C}$  were done, and  $T_g$  was determined from the midpoint of the change in the specific heat. The conversion or degree of cure,  $x$ , is related to the enthalpy released during the exothermic reaction of the epoxy-amine system. The relation is given in Equation (1), where  $\Delta H_t$  is the partial heat of reaction at a given time, and  $\Delta H_0$  is the total heat of reaction at  $t=0$  (corresponding to  $x=0$ )

$$x = 1 - \frac{\Delta H_t}{\Delta H_0} \quad (1)$$

DSC was also used to determine the  $T_g$  of the networks after the three different curing cycles. The values of  $T_g$  were used to calculate the epoxy conversion,  $x$ , through the Di Benedetto empirical model modified by Pascault and Williams [13]:

$$\frac{T_g - T_{g_0}}{T_{g_\infty} - T_{g_0}} = \frac{\lambda x}{1 - (1 - \lambda)x} \quad (2)$$

where  $T_{g_0}$  and  $T_{g_\infty}$  are the glass transition temperatures of the unreacted initial system and of the fully cured network, respectively;  $\lambda$  is the ratio of the change in heat capacity  $\Delta C_p$  at the glass transition temperature, for the fully cured and uncured states:

$$\lambda = \frac{\Delta C_{p_\infty}}{\Delta C_{p_0}} \quad (3)$$

All these values were taken from DSC runs.

### 2.2.2. Experimental setup and procedure for acoustic characterization

Two acoustic approaches were performed: the first was based on the measurement of the acoustic bulk velocities of the longitudinal and shear waves; and the second on the propagation of guided Lamb waves.

The acoustic longitudinal and shear bulk wave velocities,  $v_L$  and  $v_s$ , in the different epoxy networks were measured using the experimental setup shown in Figure 1.

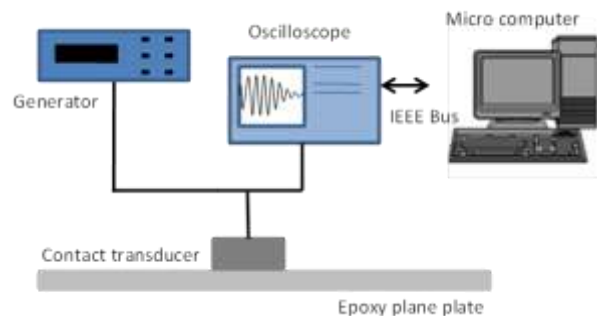


Figure 1 : Schematic diagram of experimental setup used for velocities measurements. Contact transducers: 5 MHz or 2.25 MHz; plate thickness: 2, 3, 4, or 5 mm

A contact transducer of 5 MHz central frequency for longitudinal waves and 2.25 MHz for shear waves, at normal incidence was placed on the epoxy bulk plane sample. The transducer was excited by an impulse and a temporal Fast Fourier Transform (FFT) was performed on the collected data. The velocities were obtained from the difference  $\Delta F$  between two successive peaks in the frequency spectrum, knowing the plate thickness  $d$ , and using the relation:

$$v_{L,S} = 2 d \Delta F \quad (4)$$

For better accuracy of the measured velocities, measurements were done on plane samples with different thicknesses of 2, 3, 4, and 5 mm. For each sample, the multireflected echoes received by the transducer were collected at different positions on the sample surface. This allowed the determination of averaged values of the longitudinal and shear wave velocities (using Equation 4), and their standard deviation from the whole measurements (around 20 data for each conversion).

The testing configuration for the experiments based on guided Lamb waves is shown in Figure 2. A contact transducer of 1 MHz central frequency was placed on a poly(methylmethacrylate) wedge of 45 degrees as an emitter, and a laser vibrometer was used as a receiver. A coupling gel is used between the wedge and the sample to enhance the acoustic energy transmission. The vibrometer decoder has been set to a frequency bandwidth between 0 and 2.25 MHz. The targeted modes with the selected wedge and the central frequency of the chosen transducer were the high Lamb modes orders, with the aim of confirming the theoretical predictions explained in section 3.2.2. The time-varying normal displacement of the propagating wave, sampled at 100 MHz, was collected for several positions at the surface of the sample, in the propagation direction, in 0.1 mm steps [7]. The experimental data were recorded for signal processing. A double Fast Fourier Transform (FFT) was performed on the space-time data to determine the experimental dispersion curves in the plan wavenumber-frequency space for the samples with thicknesses of 2 and 5 mm, and for the three conversions.

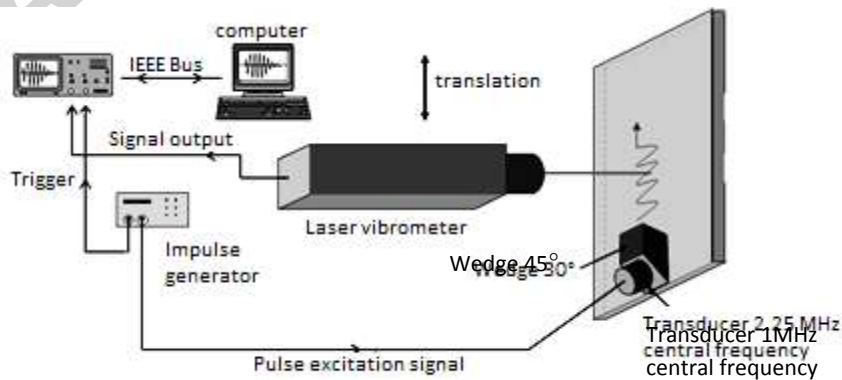


Figure 2 : Schematic diagram of experimental setup used for Lamb waves propagation in an epoxy plate, thickness: 2 or 5 mm

### 3. Results and discussion

#### 3.1. Thermal characterization

The DSC curves for the DGEBA+D230 system, obtained just after mixing at  $t=0$  and after 8 hours of reaction at room temperature, are shown in Figure 3. These curves allow the determination of the glass transition temperature,  $T_g$ , and enthalpy of reaction,  $\Delta H$ , visualized by the step in the heat flow and by the exothermic peak, respectively.

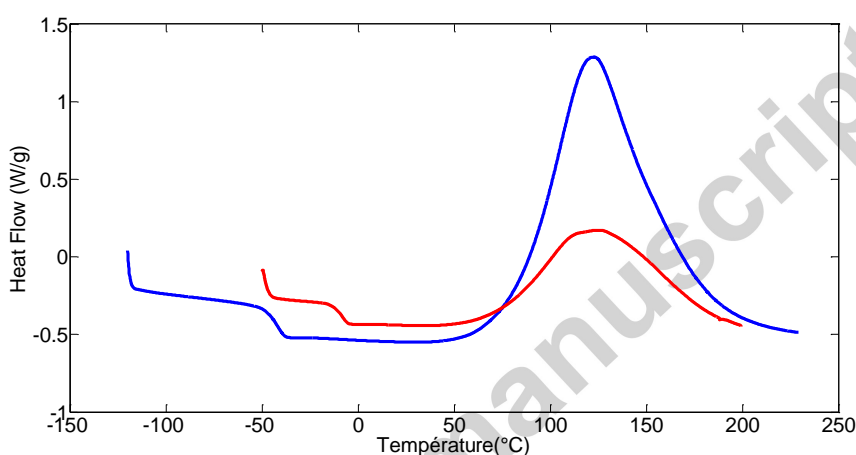


Figure 3 : Measurements of  $T_g$  and  $\Delta H$  by DSC on epoxy-amine system (DER 331 + D230) after mixing ( $t=0$ , blue curve), and after 8h of reaction at room temperature (red curve)

As expected, the glass transition temperature increases, whereas the enthalpy of the reaction peak decreases.  $T_{g0}$  is found to be equal to  $-44\text{ }^\circ\text{C}$ . The exothermic peak is observed with a maximum at  $120\text{ }^\circ\text{C}$ ;  $\Delta H_0$  is deduced from the area under the peak and is found to be equal to  $432\text{ J/g}$ ; a typical value for this type of epoxy-amine system [14]. The evolution of  $T_g$  versus time of reaction at room temperature is given in Figure 4.

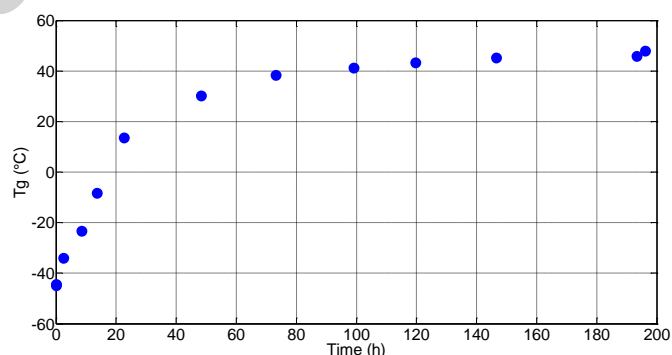


Figure 4 : Variation of glass transition temperature,  $T_g$ , measured by DSC, versus time of reaction at room temperature

A plateau is obtained after about 100 hours (approximately 4 days) at room temperature. At that point, the glass transition temperature is equal to 43°C. Figure 5 gives the evolution of the conversion,  $x$ , obtained from the residual enthalpy of reaction and Equation (1).

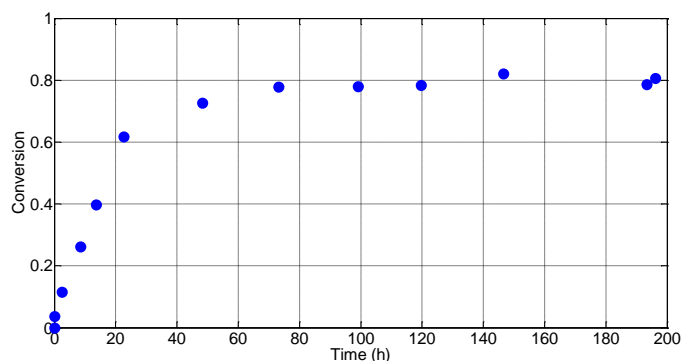


Figure 5 : Variation of epoxy conversion,  $x$ , obtained by DSC, versus time of reaction at room temperature

In this case the plateau is obtained after 50 hours at room temperature. This plateau shows that the chemical reaction is stopped by a vitrification phenomenon. The corresponding conversion is  $x=0.8$ , which is the maximum value that can be reached for a crosslinking at room temperature in our case. The gel point, which is known to occur for a theoretical conversion close to  $x=0.6$  [15], is obtained after 22 hours. The difference between the beginnings of the plateau regions can be explained by the fact that the glass transition temperature,  $T_g$ , is a more sensitive parameter than the conversion. Indeed, the determination of the conversion can be distorted at long reaction times because the phenomenon of glass transition can be superimposed on the exotherm peak (during the chemical reaction, the glass transition temperature increases, so there is interference between the jump linked to the  $T_g$  and the peak linked to the exotherm). From these experimental values, the variation of  $T_g$  versus the conversion,  $x$ , can be plotted. The point corresponding to a full conversion,  $x=1$ , has been determined on a sample cured using the third curing cycle. The interest of this plot is to be independent of time (Figure 6). In addition, the Di Benedetto plot is overlaid on the experimental data. The values reported in Table 2 were taken to draw this graph. As expected, a good agreement between the two plots is obtained.

Table 2 : Parameter values used for Di Benedetto model, obtained by DSC measurements

	$T_{g0}$ (°C)	$\Delta C_{p0}$ (J/(g.°C))	$T_{g\infty}$ (°C)	$\Delta C_{p\infty}$ (J/(g.°C))	$\lambda = \Delta C_{p\infty}/\Delta C_{p0}$
DGEBA-D230	-43	0.73	92	0.39	0.53



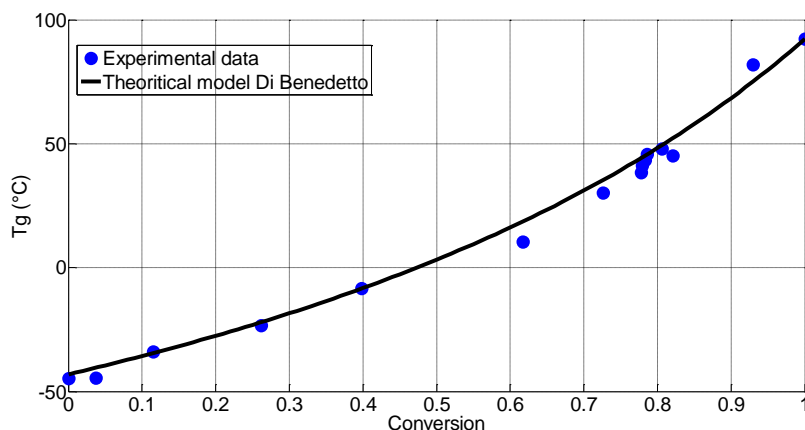


Figure 6 : Variation of glass transition temperature,  $T_g$ , versus epoxy conversion,  $x$ : (•) experimental data obtained by DSC; and (—) Di Benedetto model

Finally, DSC was used to measure the  $T_g$  of the different plates crosslinked with the three different curing cycles, and the  $T_g$  was found equal to 48°C, 83°C, and 92°C, respectively. Then, from the  $T_g$  vs. the conversion plot, the conversions were determined and found to be equal to  $x=0.8$ ,  $x=0.93$  and  $x=1$ , respectively.

It is well known that the epoxy conversion has an important influence on the network properties, particularly on mechanical behavior. In our study, the three synthesized epoxy networks (conversion equal to  $x=0.8$ ,  $x=0.93$  and  $x=1$ ) are in the glassy state at room temperature. Indeed, their glass transition temperatures are above room temperature. The Young moduli of such networks are in the range of 2–3 GPa at room temperature. Moreover, it is known that these values show a slight decrease when the conversion increases [16],[17]. Our aim is to show if these variations in epoxy conversion, i.e. in moduli, can be detected by ultrasound NDT methods.

### 3.2. Results from ultrasound analyses

#### 3.2.1. Results from velocities determination

An example of spectra obtained on the epoxy plate of 2 mm is shown in Figure 7. From the set of spectra recorded, the longitudinal and shear velocities were calculated using Equation (4). The results are presented in Table 3. Results show that even if the velocities increase with the conversion, the variations are not significant enough to distinguish the samples clearly. Indeed, one can see that shear velocity is the least sensitive to the conversion, as its variations are smaller than the standard deviation. For the longitudinal velocity, the sample of  $x=0.8$  conversion is slightly distinguished from the others, regarding standard deviation, but the samples of  $x=0.93$  and  $x=1$  conversions cannot be distinguished. Published data on the variation of velocities (compression and shear waves), measured

as a function of reaction time at room temperature on different epoxy formulations, have shown that the velocities increase very rapidly at the beginning of the reaction and rapidly reach a plateau value [12], but no correlation with conversion was established. Our experiments were done on glassy epoxy networks with  $T_g$  higher than room temperature, in which the molecular mobility is limited. In this range of high epoxy conversion ( $x \geq 0.8$ ) we can conclude that the shear bulk waves are not sensitive to variation in the epoxy conversion, whereas the longitudinal ones are more sensitive if the conversion is not too close to  $x=1$ .

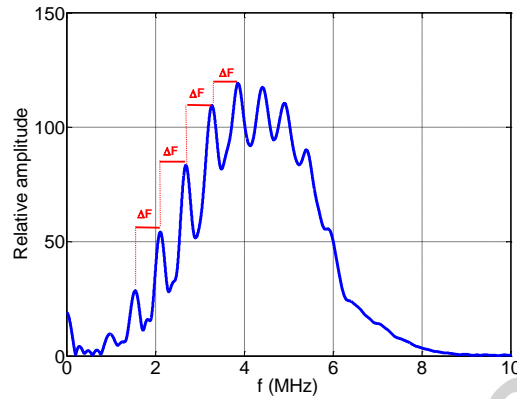


Figure 7: Typical frequency spectrum obtained after FFT on an epoxy plate of 2 mm thick and epoxy conversion of 80%

Table 3: Shear and longitudinal velocities measured for each epoxy conversion

Conversion $x$	Longitudinal		Shear	
	Velocities (m/s)	Standard deviation (m/s)	Velocities (m/s)	Standard deviation (m/s)
0.8	2441	26	1116	50
0.93	2506	38	1119	33
1	2512	30	1120	74

### 3.2.2. Results from guided Lamb waves method

Another type of experiment was conducted, based on guided Lamb waves that are used widely in nondestructive testing (NDT) and material characterization, because of their sensitivity to the material properties [8][10]. The aim is to check if some Lamb modes can be pertinent indicators of the epoxy conversion of the samples.

First, the theoretical dispersion curves of Lamb waves were determined for the three samples, using the previously measured longitudinal and shear velocities and the thickness as input data. The aim is to check the sensitivity of the different modes to small variations of the bulk shear, and longitudinal velocities due to the variation of the conversion. The dispersion curves of Lamb waves,

$k_x h$ , as a function of  $\omega h/c_T$ , where  $k_x$  is the wavenumber,  $\omega$  the angular frequency, and  $h$  the half thickness of the epoxy plate, were calculated by solving the characteristic equation obtained by a classical method, based on the free plate surfaces assumption [18],[19], for an isotropic plate. These curves are plotted in Figure 8 for the three couples of velocities corresponding to the three epoxy conversions. The single-plate modes are herein indicated using  $S_i$  for the symmetric modes and  $A_i$  for the antisymmetric modes, where  $i=0, 1, 2, \dots$  is the mode order. The lower modes  $A_0, S_0, A_1, S_1$ , and  $A_2$  are not sensitive to the conversion, whereas the high-order modes exhibit sensitivity depending on the frequency. For example, the  $S_2, A_3$ , and  $S_5$  modes depend on the conversion at low frequency, whereas  $S_3, A_4$ , and  $S_4$  depend on high frequency. Moreover, the higher the mode, the more marked the difference when the frequency increases. This theoretical analysis leads us to suppose that discrimination between the conversions of the three networks can be expected by experimental measurements.

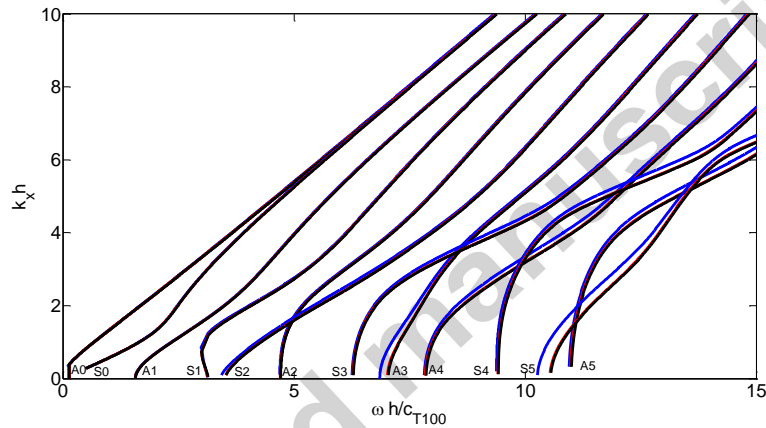


**Figure 8 : Theoretical dispersion curves of Lamb waves calculated for epoxy networks of different conversions :  $x=0.8$  (blue curve),  $x=0.93$  (red curve), and  $x=1$  (black curve). Lamb-type wave mode is identified by a letter (A: antisymmetric; S: symmetric) and a number.**

The experimental curves plotted in Figure 9 are the representation of the double FFT obtained for the epoxy plate of 2 mm thickness, for the two conversions of  $x=0.8$  (Fig. 9.a) and  $x=0.93$  (Fig. 9.b). The theoretical dispersion curves are superimposed for comparison. Figure 10 (a, b, and c) corresponds to the dispersion curves for the sample of 5 mm thickness for the three conversions. The higher excited mode for the samples of 2 mm thickness is the  $S_2$  mode, whereas  $S_2$  and  $A_4$  are excited for the samples of 5 mm thickness. One can note the good agreement between the theoretical and experimental results, which validate the accuracy of the measured longitudinal and shear velocities.

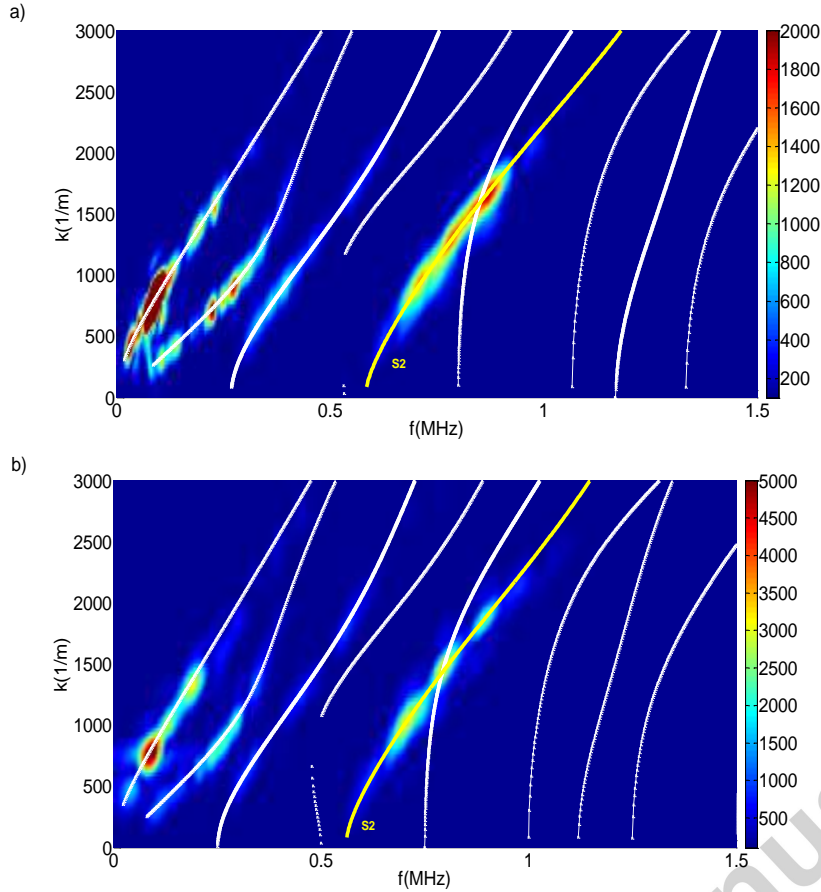


Figure 9 : Experimental Lamb-type wave dispersion curves for 2 mm-thick epoxy plate with a conversion of (a)  $x=0.8$  and (b)  $x=0.93$ , superimposed over theoretical dispersion curves (white line).

The frequency-wavenumber couples are collected on the experimental data for the S2 mode, which is the common mode obtained for all the experiments. Figure 11 shows the plotted wavenumber versus the frequency for the samples of 2 mm thickness ( $x=0.8$  and  $x=0.93$  conversions), and Figure 12 shows the same for the samples of 5 mm thickness ( $x=0.8$ ,  $x=0.93$  and  $x=1$ ). A clear differentiation between networks at  $x=0.8$  and  $x=0.93$  conversion can be observed. For a given frequency, the averaged difference between the wavenumbers for the samples of  $x=0.8$  and  $x=0.93$  conversion is about  $100 \text{ m}^{-1}$ . This difference is greater compared to the wavenumber step obtained experimentally using the spatial FFT, which is  $30 \text{ m}^{-1}$ . The S2 mode, in the used frequency range, and for this sample of 2 mm thickness, is then sensitive enough to discriminate among these conversions. Figure 12 shows also the differentiation between the three conversions for samples of 5 mm thickness, using the S2 mode, but to a lesser degree, as the difference between the wavenumbers at a given frequency is around the experimental wavenumber step. For this sample, the S2 mode is not sufficiently accurate.

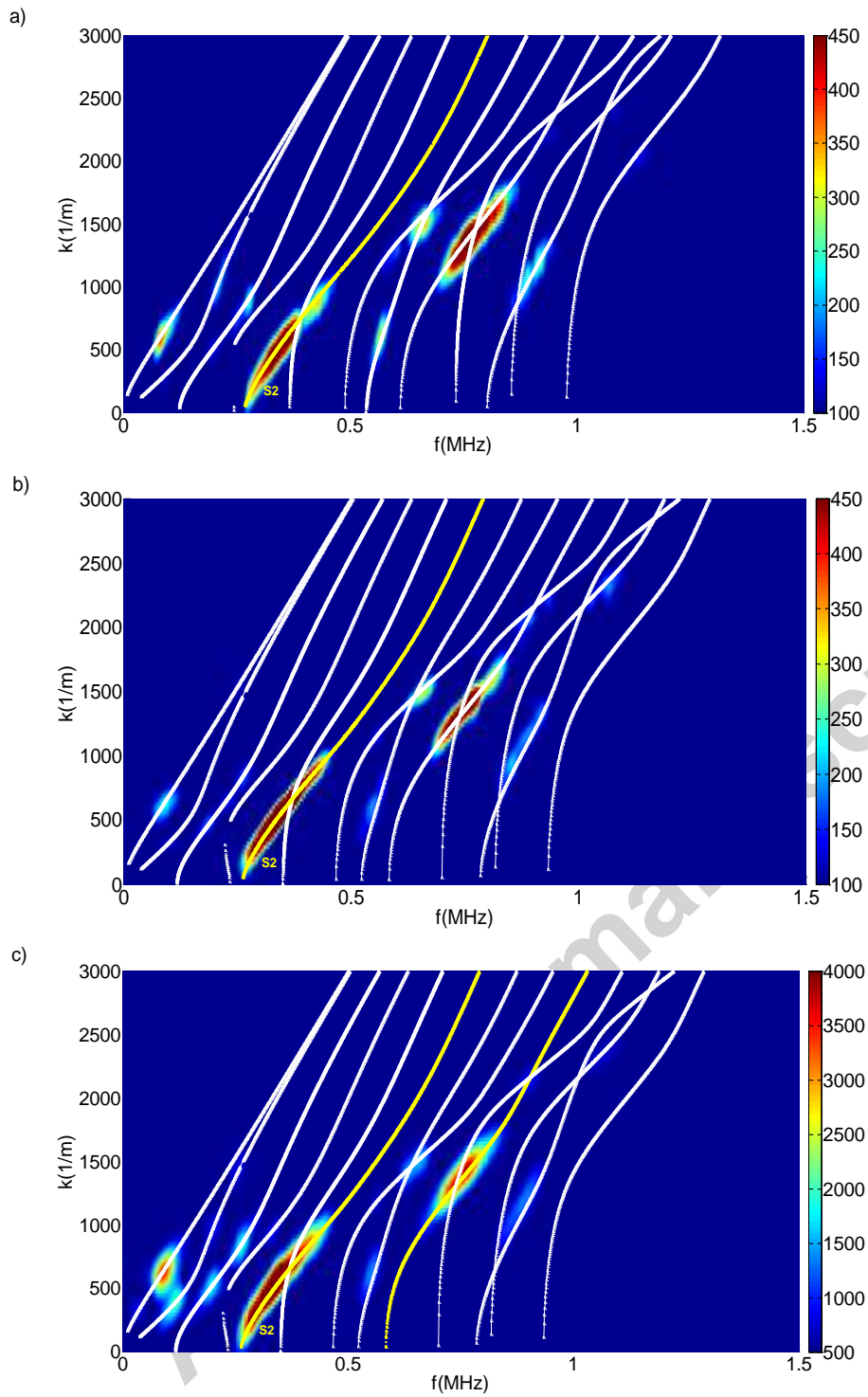


Figure 10 Experimental Lamb-type wave dispersion curves for a 5 mm-thick epoxy plate with conversion of (a)  $\chi=0.8$ , (b)  $\chi=0.93$  and (c)  $\chi=1$ , superimposed over theoretical dispersion curves (white line).

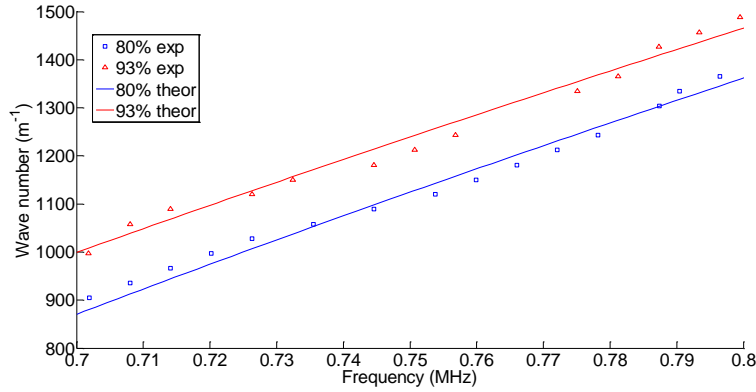


Figure 11 : Wave number versus frequency for S2 mode for 2 mm thick epoxy plate at different conversion: symbols, experimental data; line, theoretical data

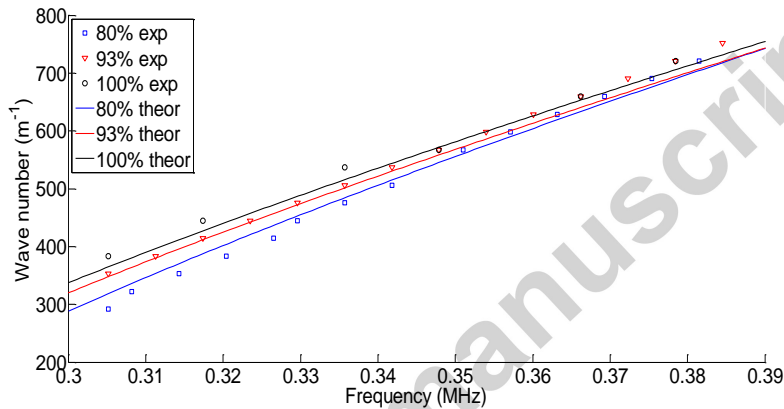


Figure 12 : Wave number versus frequency for S2 mode for 5 mm thick epoxy plate at different conversion: symbols, experimental data; line, theoretical data

A higher Lamb mode is then used. Figure 13 presents the plotted wavenumber versus frequency of the A4 mode for samples of 5 mm thickness. A better distinction is shown among the samples at  $x=0.8$  and  $x=0.93$ , or  $x=1$  conversions, as the averaged difference between wavenumbers for a given frequency is around  $100 \text{ m}^{-1}$ . One can conclude that the greater the thickness, the greater the differentiation between the conversions needs to be using higher Lamb modes. The discrimination is therefore optimal for an ad-hoc frequency-thickness product. Moreover, one can see in Figure 13 that even if the samples of  $x=0.93$  and  $x=0.1$  are discriminated, the “wavenumber-frequency” couple is close. This can be explained by the fact that the glass transition temperature  $T_g$  of the sample of  $x=0.8$  conversion equal to  $48^\circ\text{C}$  is very different from that of the samples of  $x=0.93$  and  $x=1$  conversions, which is equal to  $83^\circ\text{C}$  and  $92^\circ\text{C}$ , respectively. These values of  $T_g$  imply viscoelastic behavior similarities between samples at  $x=0.93$  and  $x=1$  conversions, and explain their significant differentiation from the sample of  $x=0.8$  conversion.

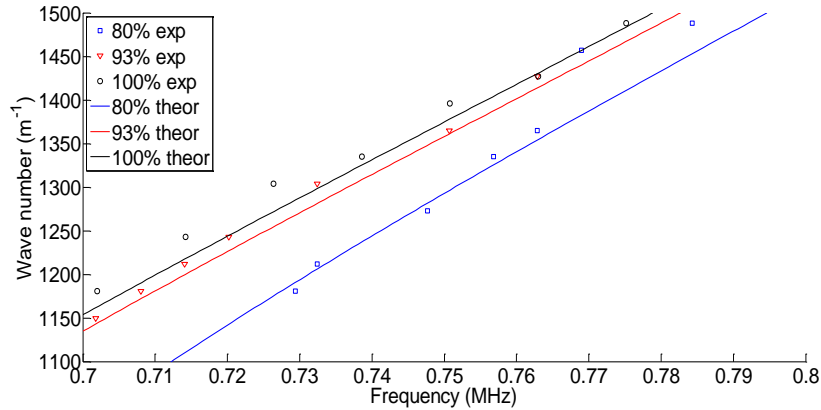


Figure 13 : Wave number versus frequency for A4 mode for 5 mm thick epoxy plate at different conversion: symbols, experimental data; line, theoretical data

#### 4. Conclusion

The aim of this work was to characterize the acoustic behavior of epoxy networks used in the field of adhesive bonding. We selected a model epoxy formulation based on a typical DGEBA monomer, cured by an aliphatic diamine. The epoxy conversion,  $x$ , also called the degree of cure, was varied by applying three different curing cycles. The relation between the conversion and curing cycle was established by conducting differential scanning calorimetry experiments. Three conversions of the epoxy networks were under consideration: two partial conversions of  $x=0.8$  (obtained via curing at room temperature) and  $x=0.93$  (obtained via a postcuring cycle); and a total conversion of  $x=1$  (obtained via a longer postcuring cycle). All networks were in the glassy state, well beyond the gel point, which occurred in this system at an epoxy conversion of  $x=0.6$ . Two ultrasonic-based methods were applied to characterize these networks. The first led to the determination of the longitudinal and shear wave velocities. A slight increase in the longitudinal wave velocities with the epoxy conversion was observed, whereas the shear wave velocities remained at a constant value. This lack of sensitivity is due to the fact that the experiments were realized on highly crosslinked networks, with high moduli. The second method was based on the propagation of Lamb waves. Indeed, a theoretical analysis leading to the plot of the dispersion curves has shown that high-order modes can be sensitive to conversion in a given frequency range. The experimental study confirmed that the S2 and A4 modes are the most pertinent ones for distinguishing the networks according to the epoxy conversion. In conclusion, our methodology, based on the proper selection of propagation modes of guided waves, is appropriate to identify partially cured networks from totally cured networks. This knowledge was used further to extend the work to an aluminum substrate/epoxy bilayer structure, where the epoxy has different conversions, and where the adhesion at the aluminum-epoxy interface was varied by applying different chemical and/or mechanical treatments to the substrate, in order to enhance the quality of the bonding progressively [20],[21].

**Acknowledgment**

The authors would like to thank the ANR (Agence Nationale de la Recherche), via the ISABEAU project (project ANR 12-BS-09-0022-01), for providing funds for the research work.

Accepted manuscript



## References

- [1] Prolongo SG, Urena A. Effect of surface pretreatment on the adhesive strength of epoxy-aluminium joints. *Int J Adhes Adhes* 2009;29:23–31.
- [2] Markatos DN, Tserpes KI, Rau E, Markus S, Ehrhart B, Pantelakis S. The effects of manufacturing-induced and in-service related bonding quality reduction on the mode-I fracture toughness of composite bonded joints for aeronautical use. *Compos Part B Eng* 2013;45(1):556–564.
- [3] Galy J, Ylla N, Moysan J, El Mahi A. Evaluation of the level of adhesion in epoxy-aluminum joints combining mechanical and NDT measurements. *Proceedings of 4<sup>th</sup> international conference on thermosets. Thermosets* 2015.
- [4] Baudot A, Moysan J, Payan C, Ylla N, Galy J, Verneret B, Baillard A. Improving adhesion strength analysis by the combination of ultrasonic and mechanical tests on single-lap joints. *The journal of Adhesion* 2014;90: 555-568.
- [5] Jordan C, Galy J, Pascault JP. Measurement of the extent of reaction of an epoxy-cycloaliphatic amine system and influence of the extent of reaction on its dynamic and static mechanical properties. *J Appl Polym Sci* 1992; 46:859–871.
- [6] Castaings M. SH ultrasonic guided waves for the evaluation of interfacial adhesion,” *Ultrasonics* 2014; 54: 1760-1775.
- [7] Predoi MV, El-Kettani MEC, Leduc D, Pareige P, Coné K. Use of shear horizontal waves to distinguish adhesive thickness variation from reduction in bonding strength. *The Journal of the Acoustical Society of America* 2015; 138(2): 1206-1213.
- [8] Ismaili NA, Chenouni D, Lakhliai Z, El-Kettani MEC, Morvan B, Izbicki JL. Determination of epoxy film parameters in a three-layer metal/adhesive/metal structure,” *IEEE Trans Ultrason Ferroelectr Freq Control* 2009; 56(9): 1955–1959.
- [9] Ismaili NA, Silva CDM, El-Kettani MEC, Despaux G, Rousseau M, Izbicki JL. Lamb modes and acoustic microscopy for the characterization of bonded structures. *Proc Meet Acoust* 2013, 19(1): 045045.
- [10] Kessler SS, Spearing SM, Soutis C. Damage detection in composite materials using Lamb wave methods. *Smart Mater. Struct.* 2002; 11(2): 269.
- [11] White SR, Mather PT, Smith MJ. Characterization of the cure state of DGEBA-DDS epoxy using ultrasonic, dynamic mechanical, and thermal probes. *Polymer Engineering and Science* 2002; 42: 51-67.
- [12] Dixon S, Jaques D, Palmer SB. The development of shear and compression elastic moduli in curing epoxy adhesives measured using non-contact transducers. *Journal of physics D: applied physics* 2003; 36: 753-759.
- [13] Pascault JP, Williams RJJ. Glass transition temperature versus conversion relationships for thermosetting polymers. *J Polym Sci Part B Polym Phys.* 1990; 28(1): 85–95.
- [14] Galy J, Sabra A, Pascault JP. Characterization of epoxy thermosetting systems by differential scanning calorimetry. *Polym Eng Sci* 1986; 26(21): 1514–1523.

- [15] Flory PJ, Principles of Polymer Chemistry. Ithaca, NY: Cornell University Press 1953.
- [16] Jordan C, Galy J, Pascault JP, Moré C, Delmotte M, Jullien H. Comparison of microwave and thermal cure of an epoxy/amine matrix. *Polym Eng Sci* 1995; 35(3): 233–239.
- [17] Burton B, Alexander D, Klein H, Garibay-Vasquez A, Pekarik A, Henkee C. Epoxy formulations using jeffamine®polyetheramines. The Woodlands, TX : Hunstmann, 2005.
- [18] H. Lamb. On waves in an elastic plate. *Proc R Soc Lond* 1917; 93(648): 114–128.
- [19] Viktorov IA, Rayleigh and Lamb waves: physical theory and applications. Plenum press 1970.
- [20] Gauthier C, El-Kettani MEC, Galy J, Predoi M, Leduc D, Izbicki JL. Lamb waves characterization of adhesion levels in aluminum / epoxy bi-layers with different cohesive and adhesive properties. *Int J Adhes Adhes* 2017;74: 15-20.
- [21] Gauthier C. Analyse acoustique et physico-chimique du couplage de solides élastiques : Etude de l'adhésion dans les collages structuraux. PhD thesis, Université du Havre, 2016.